Sensitivity analysis for ULOF of PGSFR using PAPIRUS

Sarah Kang [a], Jaeseok Heo [a], Sung Won Bae [a]*

[a]Korea Atomic Energy Research Institute, 1045 Daedeok-daero, Yuseong-gu, Daejeon 305-353, South Korea
*Corresponding author: bswon@kaeri.re.kr

1. Introduction

A prototype Gen-IV Sodium-cooled Fast Reactor (PGSFR) is a 150 MWe pool-type fast reactor designed using U-TRU-Zr metal fuel. There are several Design Extension Condition (DEC) events of PGSFR such as unprotected transient overpower (UTOP), unprotected loss of flow (ULOF), unprotected loss of heat sink (ULOHS), large partial subassembly blockage, large Steam Generator Tube Rupture (SGTR), large sodium leak and Station Black Out (SBO) as summarized in table I. It should be noted that DEC events are the accidents having probability of occurrence ranging from 10^{-8} to 10^{-6}. In this research, ULOF accident was selected after determining the Phenomena Identification and Ranking Table (PIRT). Based on the development of PIRT, the sensitivity analysis was performed to confirm the relative importance of the parameters.

2. PGSFR

The PGSFR, which is a pool type Sodium-cooled Fast Reactor (SFR), is being designed by Korea Atomic Energy Research Institute (KAERI) [1]. The heat transport system of the PGSFR consists of the primary heat transport system (PHTS) with two centrifugal type mechanical pumps including pony pumps, intermediate heat transport systems (IHTS) with four intermediate heat exchangers (IHX), two intermediate centrifugal type pumps and two steam generators and power conversion system. The decay heat removal systems

Table I: Category of Beyond Design Basis Accident (BDBA)

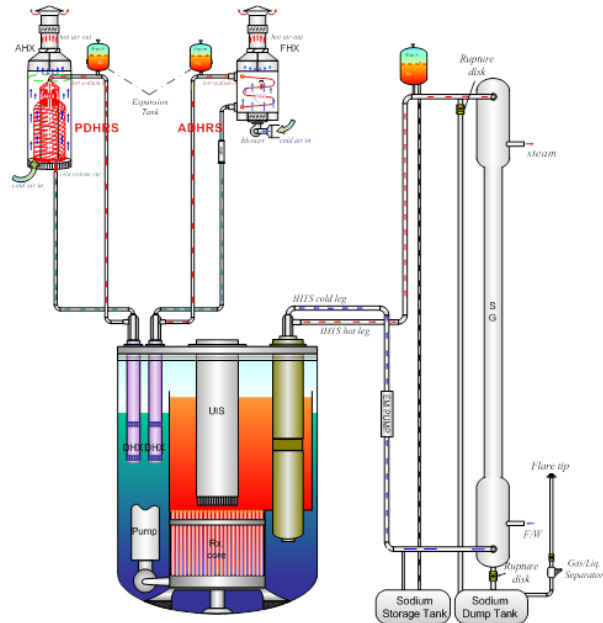| Category		Frequency / RY	Event	Acceptance criteria
BDBA	DEC	$10^{-8} \le F < 10^{-6}$	UTOP	Bounding events No fuel melting
			ULOF	
			ULOHS	No positive reactivity insertion
			Large partial subassembly blockage	
			Large sodium leak	No large radioactive release
			SBO	
	SA	$10^{-8} < F$	HCDA	No fuel melt transfer Cool-able geometry No sodium boiling No re-criticality

Fig. 1. Schematic of PGSFR

(DHRS) of PGSFR are comprised of the active decay heat removal systems (ADHRS) and passive decay heat removal systems (PDHRS) as shown in fig. 1.

3. MARS-LMR

The MARS (Multi-dimensional Analysis for Reactor Safety) code is used for the analysis of transients in water-cooled reactors [2]. To use the code for the analysis of transients in a liquid metal cooled reactor [3], liquid metal properties were newly added to this code and defined as MARS-LMR. This code has the same governing equations and solution schemes as the MARS code with specific models added including the pressure drop correlations for wire-wrapped SFR core geometry, heat transfer correlations related to liquid metal and reactivity feedback models which include the grid plate (GP) and above core load pad (ACLP) strain coefficient related to the core radial expansion reactivity feedback. Additional models that were added include the cladding strain coefficient related to the fuel axial expansion reactivity feedback, and the control rod driving line (CRDL) and reactor vessel (RV) expansion reactivity coefficient. In this research, the sources of the MARS-LMR code were revised to perform the sensitivity analysis.

4. PIRT

PIRTs are developed and commonly used as a tool to address plant behavior in the context of identifying the relative importance of systems, components, processes and phenomena for driving the plant response. However, details of PIRT development may vary depending on the specific problem to be resolved [4]. In this research, the objectives of the PIRT for the PGSFR are to evaluate the suitability of MARS-LMR model for safety analysis, the needs of revision, and the standard of the uncertainty for safety analysis code. The PIRT for the PGSFR was developed by a group of experts having the experience in design and safety analysis.

4.1 Specification of scenario

When developing the PIRT, the particular accident scenario must be identified. Based on the expert opinions, the ULOF was selected to perform the sensitivity analysis and uncertainty propagation of PGSFR system. The ULOF is a reactor accident that occurs because of pumping failure without scram. When the pump failure occurs, the reactor coolant circulation would be stopped by the active equipment after the period of the pump coastdown. Instead, natural convection due to the difference in the density generated by temperature gradients between the core and the coolant occurred. In the condition of the natural convection, the prediction of the cooling capability of the IHX determined by the temperature gradient and the velocity of the coolant affects the process of the accident scenario. The process of ULOF is almost determined by reactivity feedback. The condition are as follows.
- Point kinetics decay heat removal : ANS-94
- End of cycle (EOC) and 102% power
- Stop operating the primary two pumps
- Failure of inserting control rods
- Operation of pony pumps and four DHRS loops
- No diverse protection system (DPS)

4.2 Figure of Merit (FOM)

The FOM includes all parameters used to judge the relative importance of the phenomena [5]. ULOF means the loss of core cooling capability owing to pumping failure of the primary pump and no leaking coolant unlike pressurized water-cooled reactor (PWR). Based on expert opinions, the FOM for the ULOF of the PGSFR is the fuel solidus temperature (1250°C), clad temperature (1075°C), and sodium boiling temperature. In the case of the sodium boiling temperature, the thermal margin of vaporization, which is the difference between saturation temperature and coolant temperature at the channel exit of hot pin, was considered and the saturation temperature determined to be approximately 900°C.

Table II: System and components of PGSFR

System	Subsystem / Component
Reactor core	Core
	Fuel assembly including CRDL
	Fuel rod
Reactor vessel	PHTS pump
	PHTS
IHX	IHX shell side (Primary side)
	IHX tube side (Secondary side)
IHTS	Expansion tank
	IHTS pipe
	IHTS pump
SGS	SG tube side
	SG shell side
DHRS	ADHRS
	PDHRS

4.3 Ranking importance of components and phenomena of the PGSFR

Initially, the system and subsystem/component of PGSFR were considered to confirm the anticipated physical phenomena and those effect as shown in table II. This stage is significant where the rank of the components is decided by the objectives of the PIRT. The method to determine the relative importance of the physical phenomena and process effected to FOM is to apply the three rank scale as shown in table III. The understanding about the ranking of the relative importance is also important and is related to the knowledge-level of experts as shown in table IV. The results of the ranking importance of components and phenomena of PGSFR are shown in tables V. In these tables, the phenomena and process having both the high relative importance and knowledge level do not require additional research or experiments. However, related models in the analysis code will be verified when considering the importance of the safety analysis. The case where the phenomena and process having the highest relative importance and lowest knowledge level requires additional research or experiments as this case affects the safety analysis and the uncertainty is high. Whereas, the case having the lowest relative importance and knowledge level does not require additional research or experiments as the effect is relatively small. However, verification of the safety analysis is required in case of the low knowledge level and high uncertainty.

Table III: Ranking scale for relative importance

Rank	General description
High, H	Large effect to safety standard Need to perform the experiment and analysis having high accuracy Most important
Medium, M	Medium effect to safety standard Need to perform the experiment and analysis having accuracy 1/2 important compared to rank H
Low, L	Low effect to safety standard 1/2 important compared to rank M
N/A	Not applicable

Table IV: Knowledge-level scale

Rank	General description
High, H	Fully known, Small uncertainty
Medium, M	Partially known, Large uncertainty
Low, L	Totally unknown

5. Selection of physical models and uncertainty range related to phenomena

In this research, the model identification and ranking table (MIRT) was developed based on the PIRT developed for the SFR reactor design division at KAERI. Development of the MIRT is the process of constructing the models used to calculating the safety analysis for certain phenomena. After selecting the PIRT, a specific nuclear power plant (NPP) and frozen code, the MIRT can be used. In the ULOF, there are fifteen models for the reactor core, with four models for the PHTS and IHTS respectively as shown in table VI. The uncertainty range of each parameter indicates 2σ deviation and are determined based on the literature and expert opinions.

6. Sensitivity analysis and ranking the importance parameters

Considering the uncertainty range of the 23 parameters, the sensitivity analysis was performed for each minimum and maximum uncertainty value of the 23 parameters as well as the nominal case. The coolant temperature measured at the hot pin channel in the core was also considered based on the sensitivity coefficients by using PAPIRUS [15]. The 22 parameters, except for wall roughness (F21), were used as the multiplier. Additionally, the wall roughness (F21) was used as an input for the minimum and maximum value as shown in tables VI and VII. The maximum value of the core inlet form loss (F15) changed to 1.6 owing to the smooth simulation. After finishing the design of the PGSFR, additional sensitivity analysis will be performed. The equation of the relative sensitivity coefficient is as follows:

$$S_r = \frac{\dfrac{r - r_0}{r_0}}{\dfrac{p - p_0}{p_0}} \tag{1}$$

Fig. 2 and 3 indicate the results of the sensitivity coefficients for the range of minimum and maximum values respectively. When comparing the nominal case using PAPIRUS, the ACLP strain coefficient (F5), core radial expansion coefficient (F6), Doppler reactivity (F13), coastdown curve (F16), and core inlet form loss
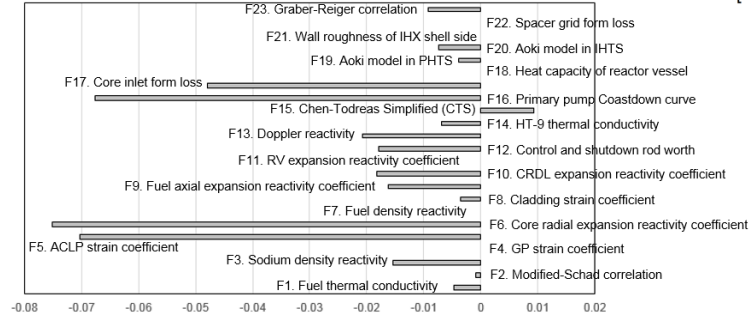

Fig. 2. Sensitivity coefficients of thermal margin of vaporization for 23 parameters having the minimum value

(F17) have the range of 1σ and were dominant as shown in the Fig. 2 and 3. Table VIII shows results of the additional sensitivity analysis based on two dominant parameters with normal distribution for the range of 2σ including the radial expansion reactivity coefficient and Doppler reactivity. The other sensitivity analysis having uniform distribution show the same results as they do not consider standard deviations unlike the normal distribution. The system of the PGSFR response was confirmed to be linear for the change of the range of two parameters. When three reactivity parameters have a minimum value such as the ACLP strain coefficient, core radial expansion coefficient, and Doppler reactivity, an increase in the fuel temperature was confirmed as the portion of returning the negative reactivity feedback decreased. When further two non-reactivity parameters also have the minimum value, primary heat transfer decreased and the fuel temperature increased. Fig. 2 indicates the comparison of the total sensitivity coefficients having the minimum value for the thermal margin of vaporization. The sensitivity coefficients of F3, F5, F6, F8, F9, F10, F12, F13 related to the negative feedback have a negative value because the coolant temperature is in an inverse proportion to the negative reactivity feedback as mentioned above. F2, F19, F20, F23 related to the primary and secondary heat transfer also have a negative value because the decrease of the cooling capability is related to the increase in the coolant temperature.
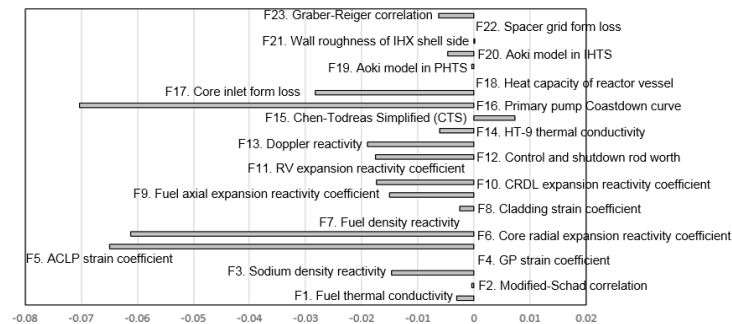

Fig. 3. Sensitivity coefficients of thermal margin of vaporization for 23 parameters having the maximum value

F16 and F17 related to the primary flowrate also have a negative value. Only F15 related to the primary pressure drop has a positive value with the same directional change as the FOM. F4, F7, F11, F18, F21, F22 cannot affect the system of the PGSFR in the uncertainty range. Fig. 3 shows the comparison of the total sensitivity coefficients that have the maximum value for the thermal margin of vaporization. The direction and dominant parameters are the same as compared to Fig. 2.

7. Conclusions

In this research, the sensitivity analysis for the ULOF of the PGSFR was performed. For 23 parameters the ACLP strain coefficient, core radial expansion coefficient, Doppler reactivity, coastdown curve, and core inlet form loss were dominant in the ULOF. Alternately, the GP strain coefficient, fuel density reactivity, RV expansion reactivity coefficient, heat capacity of reactor vessel material, wall roughness of IHX shell side, and spacer grid form loss did not affect the PGSFR system for the ULOF. The core inlet form loss should address additional sensitivity analysis.

Acknowledgement

REFERENCES

[1] K.S. Ha, Workshop for SFR inherent safety, Spring Korean Nuclear Society workshop, Jeju, Republic of Korea, 2014.
[2] J.J. Jeong, K.S. Ha, B.D. Chung, W.J. Lee, Development of a multi-dimensional thermal-hydraulic system code, MARS 1.3.1, Annals of Nuclear Energy, Vol.26, pp.1611-1642, 1999.
[3] K.S. Ha, H.Y. Jeong, C.G. Cho, Y.M. Kwon, Y.B. Lee, D.H. Han, Simulation of the EBR-II loss-of-flow tests using the MARS code, Nuclear Technology, Vol.169, pp.134-142, 2010.
[4] G.E. Wilson, B.E. Boyack, The role of the PIRT process in experiments, code development and code applications associated with reactor safety analysis, Nuclear Engineering and Design, Vol.186, pp.23-37, 1998.
[5] G.E. Wilson, Historical insights in the development of best estimate plus uncertainty safety analysis, Annals of Nuclear Energy, Vol.52, pp.2-9, 2013.

[6] NEA/CSNI/R(97)35/volume2, Report of the uncertainty methods study for advanced best estimate thermal hydraulic code applications.
[7] M.S. Kazimi, M.D. Carelli, Heat transfer correlation for analysis of CRBRP assemblies, CRBRP-ARD-0034, 1976.
[8] H. Soon, Y.I. Kim, Y.J. Kim, Analysis of BFS-73-1 experiment, KAERI/TR/1133/98.
[9] D.G. Cacuci, Handbook of nuclear engineering, Springer, New York, 2010.
[10] K.S. Ha, K.R. Lee, W.P. Chang, H.Y. Jeong, Validation of the reactivity feedback models in MARS-LMR, KAERI/TR-4395/2011.
[11] S.K. Cheng, N.E. Todreas, Hydrodynamic models and correlations for bare and wire-wrapped hexagonal rod bundles − bundle friction factors, subchannel friction factors and mixing parameters, Nuclear Engineering and Design, Vol.92, pp. 227-251, 1986.
[12] S.K. Chen, N.E. Todreas, N.T. Nguyen, Evaluation of existing correlations for the prediction of pressure drop in wire-wrapped hexagonal array pin bundles, Nuclear Engineering and Design, Vol.267, pp.109-131, 2014.
[13] S. Aoki, Current liquid-metal heat transfer research in Japan, Progress in Heat and Mass Transfer, Vol.7, pp.569-573, 1973.
[14] H. Graber, M. Rieger, Experimental study of heat transfer to liquid metals flowing in-line through tube bundles, Progress in Heat and Mass Transfer, Vol.7, pp.151-166, 1973.
[15] J. Heo, K.D. Kim, PAPIRUS, a parallel computing framework for sensitivity analysis, uncertainty propagation, and estimation of parameter distribution, Nuclear Engineering and Design, Vol.292, pp.237-247, 2015.

Table V: PIRT

System	Subsystem /Component	Phenomena	UTOP	ULOF	ULOHS	Knowledge level
Reactor core	Core	Fuel rod heat transfer	H	H	H	M
		Rate of reactivity insertion	H	N/A	N/A	H
		Coolant density effect	M	M	M	H
		Radial core expansion	H	H	H	M
	Fuel assembly including CRDL	Axial expansion of fuel and cladding	H	H	H	M
		Control rod drive line expansion	H	H	H	H
		Doppler reactivity feedback	M	M	H	H
		Inter assembly heat transfer	M	H	M	M
	Fuel rod	Core pressure drop	L	H	L	H
		Fission gas generation	L	L	L	M
		Fuel-clad eutectic formation	L	L	L	M
Reactor vessel (RV)	PHTS pump	Pump coastdown	N/A	H	N/A	M
		Pump heat generation	L	L	M	H
	PHTS	Natural circulation (1D global flow)	N/A	H	N/A	M
		Primary system pressure drop	L	H	L	H
		Thermal stratification	L	L	L	M
		Reactor vessel heat loss	L	M	M	L
		Internal heat structure heat transfer	L	H	L	H
		3D flow in reactor vessel	L	M	L	M
IHX	IHX tube side (Secondary side)	Tube side pressure drop	L	L	L	H
		Tube side heat transfer	H	H	M	H
	IHX shell side (Primary side)	Shell side pressure drop	L	M	L	H
		Shell side heat transfer	H	H	M	H
IHTS	Expansion tank	Sodium volume expansion	N/A	N/A	N/A	H
	IHTS pipe	Pressure drop	L	L	L	H
	IHTS pump	EM pump characteristic curve	N/A	N/A	N/A	M
SGS	SG tube side	SG tube heat transfer	H	H	H	L
	SG shell side	SG shell heat transfer	H	H	L	H
DHRS	ADHRS	Blower characteristic curve	L	L	M	H
		EM pump characteristic curve	L	L	M	M
		FHX air tube heat transfer	L	L	H	M
		FHX air shell heat transfer	L	L	H	H
		DHX Na-Na tube heat transfer	L	L	H	H
		DHX Na-Na shell heat transfer	L	L	H	H
	PDHRS	AHX air tube heat transfer	L	L	H	H
		AHX air shell heat transfer	L	L	H	M
		DHX Na-Na tube heat transfer	L	L	H	H
		DHX Na-Na shell heat transfer	L	L	H	H
		Natural circulation	L	L	H	M

Table VI: MIRT

System	Phenomena			Related model	Distribution function	Uncertainty band [2σ]
Reactor core	Fuel rod heat transfer		F1	Fuel conductivity	Normal	± 0.58 W/m·K
			F2	Convection	Normal	± 20%
	Coolant density effect		F3	Sodium density reactivity	Normal	± 32.6%
	Core radial expansion		F4	GP strain coefficient	Uniform	± 10%
			F5	ACLP strain coefficient	Uniform	± 10%
			F6	Reactivity coefficient	Normal	± 30.6%
	Axial expansion of fuel and cladding		F7	Fuel density reactivity	Uniform	± 10%
			F8	Cladding strain coefficient	Uniform	± 10%
			F9	Reactivity coefficient	Normal	± 30.6%
	Control rod drive line expansion		F10	CRDL expansion reactivity coefficient	Uniform	± 10%
			F11	RV expansion reactivity coefficient	Uniform	± 10%
			F12	Control and shutdown rod worth	Normal	± 19.8%
	Doppler reactivity feedback		F13	Doppler reactivity	Normal	± 30%
	Inter assembly heat transfer		F14	HT-9 conduction	Uniform	± 10%
	Core pressure drop		F15	Friction model	Normal	± 30%
Primary heat transfer system (PHTS)	Pump coastdown		F16	Coastdown curve	Uniform	± 10%
	Natural convection		F17	Core inlet form loss	Log-uniform	0.5 – 2.0
	Internal structure heat transfer		F18	Heat capacity	Uniform	± 10%
			F19	Convection	Normal	± 20%
Intermediate heat transfer system (IHTS)	Tube side heat transfer		F20	Convection	Normal	± 20%
	Shell side pressure drop		F21	Wall roughness	Uniform	$10^{-5} – 2.0 \times 10^{-4}$
			F22	Spacer grid form loss	Uniform	0.5 – 1.5
	Shell side heat transfer		F23	Convection	Normal	± 12.2%

Table VII: Sensitivity analysis results of thermal margin of vaporization

Number	Related model	Distribution function	Thermal margin of vaporization			
			Min (K)	S_r	Max (K)	S_r
F1	Fuel conductivity	Normal	0.0	-0.0048	-0.1	-0.0030
F2	Convection	Normal	0.0	-0.0009	-0.1	-0.0004
F3	Sodium density reactivity	Normal	2.8	-0.0154	-2.8	-0.0146
F4	GP strain coefficient	Uniform	0.0	0.0	0.0	0.0
F5	ACLP strain coefficient	Uniform	8.0	-0.0702	-7.5	-0.0650
F6	Reactivity coefficient	Normal	12.4	-0.0751	-11.3	-0.0612
F7	Fuel density reactivity	Uniform	0.0	0.0	0.0	0.0
F8	Cladding strain coefficient	Uniform	0.3	-0.0035	-0.4	-0.0026
F9	Reactivity coefficient	Normal	2.7	-0.0161	-2.8	-0.0150
F10	CRDL expansion reactivity coefficient	Uniform	2.0	-0.0182	-2.0	-0.0173
F11	RV expansion reactivity coefficient	Uniform	0.0	0.0	0.0	0.0
F12	Control and shutdown rod worth	Normal	2.0	-0.0179	-2.0	-0.0175
F13	Doppler reactivity	Normal	3.5	-0.0208	-3.4	-0.0191
F14	HT-9 conduction	Uniform	0.7	-0.0069	-0.8	-0.0061
F15	Friction model	Normal	-1.7	0.0092	1.2	0.0072
F16	Coastdown curve	Uniform	7.9	-0.0676	-8.2	-0.0702
F17	Core inlet form loss	Log-uniform	27.5	-0.0478	-19.5	-0.0283
F18	Heat capacity	Uniform	0.0	0.0	0.0	0.0
F19	Convection	Normal	0.3	-0.0039	-0.4	-0.0004
F20	Convection	Normal	0.7	-0.0074	-0.6	-0.0048
F21	Wall roughness	Uniform	0.0	0.0	0.0	0.0001
F22	Spacer grid form loss	Uniform	0.0	0.0	0.0	0.0
F23	Convection	Normal	0.5	-0.0092	-0.6	-0.0064

Table VIII: Dominant parameters for ULOF of PGSFR

Number	Related model	Distribution function	1σ		2σ	
			Thermal margin of vaporization			
			Min (K)	Max (K)	Min (K)	Max (K)
F5	ACLP strain coefficient	Uniform	54.9	70.5	54.9	70.5
F6	Reactivity coefficient	Normal	50.5	74.2	36.5	84.5
F13	Doppler reactivity	Normal	59.4	66.3	55.8	69.6
F16	Coastdown curve	Uniform	54.6	71.4	54.6	71.4
F17	Core inlet form loss	Log-uniform	34.8	82.5	34.8	82.5